International Journal of Mass Spectrometry and Ion Physics, 38 (1981) 323—331 323
Elsevier Scientific Publishing Company, Amsterdam — Printed in The Netherlands

29

UNIMOLECULAR KINETICS OF PYRIDINE ION FRAGMENTATION *

HENRY M. ROSENSTOCK, ** ROGER STOCKBAUER *** and ALBERT C. PARR **

National Measurement Laboratory, National Bureau of Standards, Washington, DC 20234 (U.S.A.)

(Received 9 August 1980)

ABSTRACT

The fragmentation of the pyridine ion to form $C_4H_4^+$ and HCN has been studied by means of photoelectron—photoion coincidence mass spectrometry with variable ion-source residence time. A detailed analysis of the time-dependent breakdown curves leads to a $T = 0$ K fragmentation threshold of 12.15 ± 0.02 eV, $\Delta H^0_{f_0}(C_4H_4^+) = 1195 \pm 12$ kJ mol^{-1}, somewhat higher than the value reported by Eland et al. The fragmentation process requires a tight transition state, in agreement with earlier conclusions of Eland et al. There is some disagreement with earlier work on the energy-dependence of the fragmentation rate. It is suggested that this may be due to distortion of the thermal vibrational population distribution of the ion after vertical ionization.

INTRODUCTION

The quantitative description of the fragmentation of large excited polyatomic ions requires knowledge of the energy threshold for the fragmentation as well as the energy-dependence of the fragmentation rate constant. In many instances, the experimental determination of threshold energy is impeded by the slow kinetics of the fragmentation, i.e., the kinetic shift of the appearance energy [1,2]. In recent years this difficulty has been attacked by means of a number of new experimental approaches and refinements in the analysis of accessible experimental information. These include studies of the effect of ion-source residence times on appearance energies [3—6], comparison and analysis of the appearance energies of a fragment and its corresponding metastable transition [7], and analysis of the effects of thermal energy and/or fragmentation kinetics on the form of the fragment-ion yield curves [7—11]. Also, a new class of experiments has been developed in which the energy imparted to the ion is specified within more or less narrow limits by means of charge exchange [12,13], by photoionization events producing photoelectrons of known energy from photons of known energy

* Dedicated to Professor Hans D. Beckey on the occasion of his sixtieth birthday.
** Radiation Physics Division.
*** Surface Science Division.

[14–21], or by use of first-derivative photon impact [22–24] or second-derivative electron impact [25,26] techniques. Although the experimental information is significantly better defined in these more recent experiments, there still remain some ill-understood complexities and attendant simplifying assumptions which are made in the analysis and quantitative interpretation of the accessible experimental information. These difficulties are often revealed when comparing different experiments which should give the same information, or when studying several molecules which provide information in an overdetermined manner, such as the heat of formation of a given ion from several precursors. Pertinent examples include collisional energy transfer in charge exchange [27,28], autoionization in first-derivative photoionization [24] and second-derivative electron impact experiments, and proper averaging of unimolecular rate constants [24,29].

In this paper we report a study of the pyridine ion fragmentation process $C_5H_5N^+ \rightarrow C_4H_4^+ + HCN$ by means of photoelectron–photoion coincidence with variable ion-source residence time [30]. This process was recently studied by Eland and co-workers [24], who used a different type of coincidence apparatus and also studied the metastable transition by first-derivative photoionization techniques. They determined a value for the fragmentation threshold and also arrived at an energy-dependence for fragmentation rates in the range $\sim 10^4$–10^7 s^{-1}.

EXPERIMENTAL

The experimental data were obtained using the threshold photoelectron–photoion coincidence mass spectrometer described previously [31]. The sample gas is ionized by a monochromatic photon beam. The resulting photoelectrons are drawn out by a weak field and filtered through a steradiancy analyzer and a cylindrical-sector energy analyzer so that only electrons having near-zero initial energy are detected. Following detection of such an electron, a drawout pulse is applied to the ion source region and the positive ion is accelerated through an accelerating–focussing lens system and a drift region. It is detected by an electron multiplier, in delayed coincidence with the electron pulse. The ion mass is determined by its time of flight, using standard electronic techniques. The electron-filtering arrangement ensures that the excitation energy of the ion is known accurately, if the ionization potential of the molecule is known accurately. The actual narrow distribution of ion internal energies sampled in this system is established by studying the electron collection efficiency above the Kr $^2P_{1/2}$ ionization threshold [31]. The half-width of this distribution is 28 meV and it is not symmetrical, having a pronounced high-energy tail resulting from some acceptance of higher-energy electrons which are initially directed towards the electron filter. Consequently, the excitation-energy sampling function has a low-energy tail [30].

The *nominal* parent-ion residence time in the source region is determined

by the ejected photoelectron transit-time to the electron multiplier and the turn-on and risetime of the drawout pulse. This time is at minimum 0.70 μs and can be increased by deliberately delaying the application of the drawout pulse. In the present experiment, nominal times of 0.70 and 5.70 μs were employed. The *actual* effective residence times are slightly longer, due to a variety of effects which have been discussed in detail elsewhere [28]. These effective residence times were 0.805 and 5.925 μs, with an estimated uncertainty of at most 0.05 μs. The effect of this uncertainty has already been discussed [29]. Time-of-flight spectra and breakdown curves were obtained in the usual manner for both effective residence times.

RESULTS AND DISCUSSION

The breakdown curves for the fragmentation are shown in Fig. 1 for both effective residence times. They exhibit a pronounced time-dependence as a result of the slow fragmentation kinetics near threshold. Also the experimentally observable onset of fragmentation lies more than 0.3 eV above the fragmentation threshold determined from our analysis of the results (see arrow in Fig. 1).

The results were analyzed in the same manner as previously [28—30]. Briefly, the rate—energy dependence was calculated for several sets of activation energies and equivalent T = 1000 K entropies. For each set a breakdown curve was calculated for the two residence times and convoluted with the

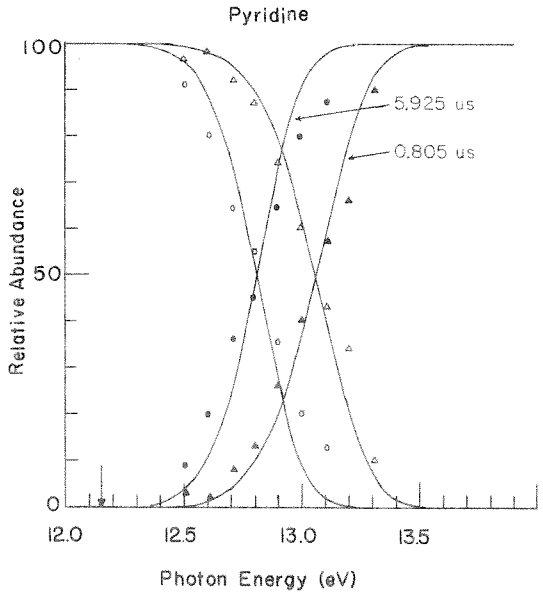

Fig. 1. Breakdown curves for pyridine ion for 5.925 and 0.805 μs effective residence times. Experimental points: ○, △, $C_5H_5N^+$ parent; ●, ▲, $C_4H_4^+$ fragment; ———, best-fit calculations. The vertical arrow indicates the thermochemical threshold.

apparatus sampling-function and the internal thermal-energy distribution. Both the presence and absence of external rotational energy in the available fragmentation energy were considered [28]. The calculations were then used to determine the photon energies at which 50% fragmentation occurred at long residence time (crossover energy) and the shift in this crossover energy on going to short residence time. In Fig. 2 is shown the dependence of this crossover energy and shift on the two significant transition-state parameters, i.e., the activation energy and the 1000-K equivalent activation entropy. From this sensitivity plot the values for the parameters that best reproduce the experimental crossover and shift are readily determined. These experimental quantities can be determined with a precision of ±0.02 eV or better. Frequencies for the pyridine ion were assumed to be identical to those for the pyridine molecule [32], and the transition-state frequencies were modeled by setting five nitrogen-dependent normal modes equal and variable, and setting a sixth nitrogen-dependent mode of 1030 cm^{-1} equal to the reaction coordinate. The reaction multiplicity was taken equal to 2.

On the assumption that the external rotations do not contribute to available fragmentation energy, the best transition-state parameters are E_{act} = 2.90 ± 0.02 eV and a 1000-K equivalent entropy of activation of 5.6 ± 0.5 cal mol^{-1}. If it is assumed that rotational energy is available, the values are E_{act} = 2.93 ± 0.02 eV and ΔS_{1000} = 5.6 ± 0.5 cal mol^{-1}. We consider the latter alternative less likely, since the activation entropy is so small (equivalent to an Arrhenius factor A of ~2.1×10^{14} s^{-1} at 1000 K) that the transition state is comparatively tight. Hence the moments of inertia in the transition state are not very different from those of the reactant ion, and external rotational energy would not be available.

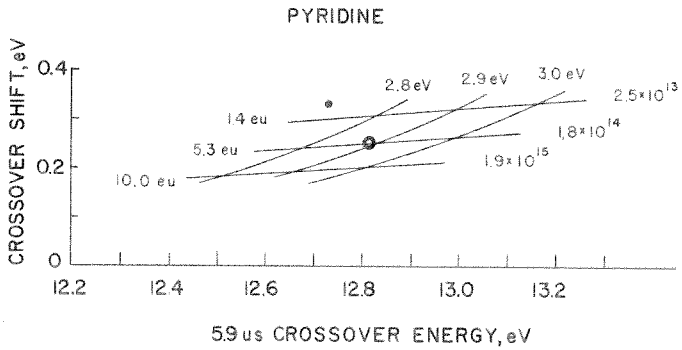

Fig. 2. Sensitivity of the pyridine ion breakdown curves to the activation energy, E_{act}, and equivalent activation entropy, $\Delta S^{\ddagger}$. The near-horizontal lines show the change of the crossover energy and crossover shift with activation energy at constant entropy; the inclined curves show the change with activation entropy at constant energy. The values of the equivalent activation entropy (calculated at 1000 K) are given in units of cal mol^{-1} $degree^{-1}$ on the left and the equivalent 1000-K Arrhenius factor A $[(kT/h) \cdot e^{\Delta S/R}]$ on the right. The present experimental results are indicated by the open circle (○) and those implied by the results of Eland et al. by the closed circle (●).

TABLE 1

Thermochemistry for pyridine fragmentation

Species	$\Delta H_{f_{298}}$ (kJ mol^{-1})	Ref.	$\Delta H^0_{f_0}$ (kJ mol^{-1})	Ref.
C_5H_5N	141.4 ± 1.2	35	158.2 ± 1.2	a
$C_5H_5N^+$	—		1051 ± 2	b
HCN	—		135.52 ± 8.37	34
$C_4H_4^+$	—		~1197	11
$C_4H_4^+$	—		1159—1180	24
$C_4H_4^+$	—		1195 ± 12	this work

[a] Converted to $T = 0$ K using vibrational frequencies given in ref. 32 and appropriate enthalpy functions, ref. 34. These room-temperature and zero-kelvin values are slightly higher (~1 kJ mol^{-1}) than the values used by Eland et al., which were taken from ref. 38.
[b] Based on an ionization potential of 9.25 eV as given by Eland et al. [24].

The activation energy of 2.90 ± 0.02 eV, combined with the ionization potential of pyridine, 9.25 eV [24] and other thermochemical values, leads to $\Delta H^0_{f_0}(C_4H_4^+) = 1195 \pm 12$ kJ mol^{-1}. The details are given in Table 1. The value for the $C_4H_4^+$ heat of formation determined in this work is somewhat higher (by ~25 kJ mol^{-1}) than that determined by Eland et al. [24] but is in surprisingly good agreement with our earlier estimate based on an analysis of the fragmentation of the benzene ion [10]. This agreement is somewhat fortuitous since the earlier estimate was based largely on reasoning by analogy. The results may also be compared to an appearance energy of 12.34 ± 0.1 eV determined by means of monoenergetic electron impact [33]. The results of the present study lead to a $T = 0$ K threshold of 12.15 ± 0.02 eV and an observed fragmentation threshold of ~12.4 eV at 5.9 μs residence time. This suggests that the ion-source residence time is considerably longer in the electron monochromator apparatus, as noted previously [33].

The present results can be compared more closely with those of Eland et al. [24]. For this purpose it is useful to examine the rate—energy dependence of the fragmentation process and to discuss critically the deviations from exact fit of the calculated and experimental breakdown curves shown in Fig. 1.

The rate—energy dependence for the fragmentation process is shown in Fig. 3. Both the present results and the earlier results of Eland et al. are shown. It is seen that the present results lie within the rather large error bounds of the earlier coincidence study. The energy-dependence is somewhat steeper here than in the earlier work. The significant deviation occurs at low energy, where our results indicate a significantly lower rate constant than that obtained in the earlier study. The earlier results at low energy (cross-hatched boxes) were based on an analysis of the first derivative of the smoothed photoionization-yield curve for the metastable transition. That analysis was

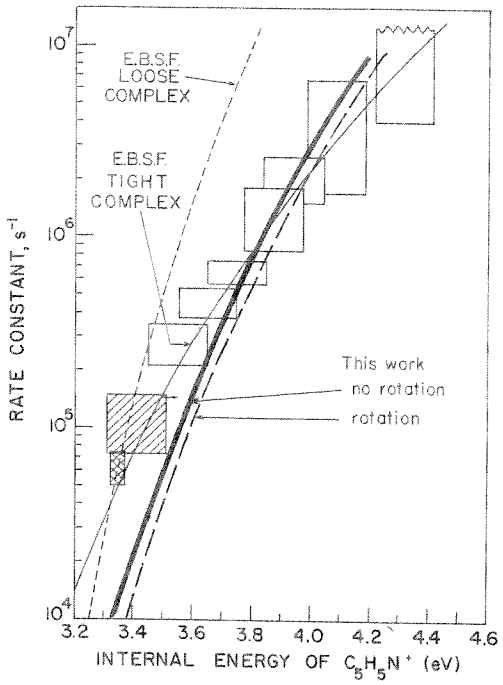

Fig. 3. Rate—energy curves for pyridine fragmentation: — — — and ▬▬, this work; - - - - - - and ———, best-fit results of Eland et al. [24]; □, individual rates determined by Eland et al. from coincidence data; ▨, individual rates determined by Eland et al. from analysis of photoionization metastable transition.

done by determining the unimolecular rate constant at which maximum collection efficiency for the metastable species would occur in the mass spectrometer configuration employed, determining the photon energy at which this maximum was observed, and approximately correcting for the energy distribution of the ion.

The energy distribution of the ion was assumed in that analysis to have a form similar to that of a classical three-dimensional rotor with a mean thermal energy of ~0.1 eV. From this an average lifetime was computed taking into account the energy-dependence of the decomposition rate. If the distribution were broader than the rotor distribution, the energy-scale correction would be larger than 0.1 eV.

Our own results and analysis may also be examined more critically. Inspection of Fig. 1 shows that the experimental transition from parent to fragment occurs over a slightly larger energy range than is calculated, particularly at the longer effective residence time. This would suggest that the rate—energy dependence is more gradual than we deduced. However, such an assumption leads to a significant disagreement when the residence-time dependence of the crossover energy is calculated. This can be illustrated as

follows. We used the best-estimate rate—energy curve determined by Eland (curve labeled E.B.S.F. Tight Complex in Fig. 3) to calculate the crossover energy and shift as it would be observed in our apparatus. The result, shown in Fig. 2 (closed circle), lies significantly outside our error bounds for the crossover.

Returning once again to the study of Eland et al., one notes that their analysis accounted for the position and form of the metastable transition as well as the coincidence—time-of-flight data. However, their experimental breakdown curves cross over at somewhat higher energies than calculated from their rate—energy curve. This deviation accords qualitatively with the slightly higher activation energy and steeper rate—energy dependence determined in the present work.

There is one more unrecognized factor which can affect the analysis of the time-dependence and form of the breakdown curve, as well as the energy-scale correction of the maximum of the photoionization metastable species. This factor is the transformation of the thermal vibrational population distribution of a molecule upon vertical ionization.

At room temperature only two-thirds of the molecules are in the vibrational ground state; the rest populate excited vibrational levels. The average thermal vibrational energy is ~0.041 eV. When the molecule is ionized this distribution is preserved in detail only if the final-state geometry and force constants are identical to those of the initial state. However, the photoelectron ion state which lies at the energy corresponding to the fragmentation threshold has not only a fairly well-resolved vibrational structure [35], but the onset of this photoelectron band shows a distinct low-energy tail extending more than 0.1 eV below the onset of the resolved vibrational structure. The latter can be interpreted as an envelope of hot-band transitions. Turner [37] has noted than ten of the normal modes are of A_1 symmetry and hence have Franck—Condon-allowed vibrational transitions upon vertical ionization if the ion state is also of symmetry C_{2v}. However, it is likely that σ ionization is involved [38], making additional normal-mode transitions allowed. At the very least, there are two A_1 modes, having frequency 602 cm^{-1} and 991 cm^{-1} with room-temperature populations of 5.5% and 1%, respectively. These populations are surely perturbed by vertical ionization. In fact, the well-resolved 560 cm^{-1} progression in the photoelectron band may correspond to the 602 cm^{-1} normal mode in the molecule.

To summarize, conditions are such as to make distortion of the thermal vibrational population likely, leading to a broadened distribution with a higher mean energy. Such an effect could account for the broader parent—daughter transition region in the breakdown curve, and would imply a correction of somewhat greater magnitude to the effective energy scale for the metastable transition observed in photoionization. The result of Eland et al. and the present work imply a correction of nearly 0.1 eV.

The above considerations suggest that the true value of the $C_4H_4^+$ heat of formation lies somewhere between the values obtained by Eland et al. and in the present work.

In connection with the problem of benzene ion fragmentation, the present results, along with those of Eland et al. [24] and our earlier study of allene [30], confirm the earlier suggestion that the two thermochemical thresholds for benzene-ion skeletal fragmentation are the same or very nearly so. Together with earlier work on the heats of formation of phenyl and benzyne [39] ions, the thermochemistry of the four major benzene ion fragmentation paths is now well established.

CONCLUSIONS

The analysis of the time-dependence of the pyridine ion breakdown curve leads to kinetic parameters somewhat different from those determined in an earlier study by Eland et al. [24]. Our results lead to a somewhat steeper energy-dependence of the unimolecular fragmentation rate constant, and are in significant disagreement with the result obtained by kinetic analysis of the metastable transition observed in photoionization. We conclude that the true value of $\Delta H^0_{f_0}(C_4H_4^+)$ lies somewhere between our value of 1195 ± 12 kJ mol^{-1} and the earlier value 1170 ± 10 kJ mol^{-1} reported by Eland et al. [24]. Evidence is presented that the vibrational thermal energy distribution of the molecule may be distorted upon vertical ionization. The transition state for the fragmentation process is tight, with a small activation entropy.

ACKNOWLEDGEMENTS

We would like to thank Dr. J. Berkowitz for sending us detailed information about his photoionization study of pyridine. Partial support of this work by the U.S. Department of Energy, Office of Environment, Contract No. 80EV10373.000, is gratefully acknowledged.

REFERENCES

1 L. Friedman, F.A. Long and M. Wolfsberg, J. Chem. Phys., 26 (1956) 714.
2 W.A. Chupka, J. Chem. Phys., 30 (1959) 191.
3 M.L. Gross, Org. Mass Spectrom., 6 (1972) 327.
4 C. Lifshitz, A.M. Peers, M. Weiss and M.J. Weiss, Adv. Mass Spectrom., 6 (1974) 871.
5 S. Gordon and N.W. Reid, Int. J. Mass Spectrom. Ion Phys., 18 (1975) 379.
6 M.A. Baldwin, Org. Mass Spectrom., 14 (1979) 601.
7 I. Hertel and Ch. Ottinger, Z. Naturforsch., 22a (1967) 40.
8 P.M. Guyon and J. Berkowitz, J. Chem. Phys., 54 (1971) 1814.
9 W.A. Chupka, J. Chem. Phys., 54 (1971) 1936.
10 H.M. Rosenstock, J.T. Larkins and J.A. Walker, Int. J. Mass Spectrom. Ion Phys., 11 (1973) 309.
11 K.E. McCulloh and V.H. Dibeler, J. Chem. Phys., 64 (1976) 4445.
12 E. Gustafsson and E. Lindholm. Ark. Fys., 18 (1960) 219.
13 B. Andlauer and Chr. Ottinger, Z. Naturforsch., 27a (1972) 293.
14 B. Brehm and E. von Puttkamer, Z. Naturforsch., 22a (1967) 8.
15 D. Villarejo, R.R. Herm and M.G. Inghram, J. Chem. Phys., 46 (1967) 4995.

16 W.B. Peatman, T.B. Borne and E.W. Schlag, Chem. Phys. Lett., 3 (1969) 492.
17 R. Stockbauer and M.G. Inghram, J. Chem. Phys., 54 (1971) 2242; R. Stockbauer, J. Chem. Phys., 58 (1973) 3800.
18 C.J. Danby and J.H.D. Eland, Int. J. Mass Spectrom. Ion Phys., 8 (1972) 153.
19 A.S. Werner and T. Baer, J. Chem. Phys., 62 (1975) 2900.
20 C.F. Batten, J.A. Taylor and G.G. Meisels, J. Chem. Phys., 65 (1976) 3316.
21 J. Dannacher and J. Vogt, Helv. Chim. Acta, 61 (1978) 361.
22 H. Hurzeler, M.G. Inghram and J.D. Morrison, J. Chem. Phys., 27 (1957) 313; 28 (1958) 76.
23 W.A. Chupka, in C. Sandorfy, P.J. Ausloos and M.B. Robin (Eds.), Chemical Spectroscopy and Photochemistry in the Vacuum Ultraviolet, D. Reidel, Boston, 1974.
24 J.H.D. Eland, J. Berkowitz, H. Schulte and R. Frey, Int. J. Mass Spectrom. Ion Phys., 28 (1978) 297.
25 J.D. Morrison, Rev. Pure Appl. Chem., 5 (1955) 22.
26 C. Lifshitz, M. Weiss and S. Landau-Gefen, Paper presented at the 25th Ann. Conf. on Mass Spectrometry and Allied Topics, Washington, DC, June, 1977.
27 J.H.D. Eland and H. Schulte, J. Chem. Phys., 62 (1975) 3825.
28 H.M. Rosenstock, R. Stockbauer and A.C. Parr, J. Chem. Phys., 73 (1980) 773.
29 H.M. Rosenstock, R. Stockbauer and A.C. Parr, J. Chem. Phys., 71 (1979) 3708.
30 R. Stockbauer and H.M. Rosenstock, Int. J. Mass Spectrom. Ion Phys., 27 (1978) 185.
31 R. Stockbauer, Int. J. Mass Spectrom. Ion Phys., 25 (1977) 89.
32 L.M. Sverdlov, M.A. Kovner and E.P. Krainov, Vibrational Spectra of Polyatomic Molecules, Wiley, New York, 1974.
33 H.M. Rosenstock, K.E. McCulloh and F.P. Lossing, Int. J. Mass Spectrom. Ion Phys., 25 (1977) 327.
34 D.R. Stull and H. Prophet, JANAF Thermochemical Tables, 2nd edn., NSRDS—NBS 37, U.S. Department of Commerce, June 1971.
35 J.B. Pedley and J. Rylance, Sussex—Natl. Phys. Lab. Computer-Analyzed Thermochemical Data: Organic and Organometallic Compounds, University of Sussex, 1977.
36 D.W. Turner, C. Baker, A.D. Baker and C.R. Brundle, Molecular Photoelectron Spectroscopy, Wiley—Interscience, New York, 1970, fig. 12.2.
37 D.W. Turner, C. Baker, A.D. Baker and C.R. Brundle, Molecular Photoelectron Spectroscopy, Wiley—Interscience, New York, 1970, p. 324 ff.
38 C. Batich, E. Heilbronner, V. Hornung, A.J. Ashe III, D.T. Clark, U.T. Cobley, D. Kilcast and I. Scanlan, J. Am. Chem. Soc., 95 (1973) 928.
39 H.M. Rosenstock, R. Stockbauer and A.C. Parr, J. Chim. Phys., 77 (1980) 745.
40 T. Baer, G. Willett, D. Smith and J.S. Phillips, J. Chem. Phys., 70 (1979) 4076.
41 G.S. Hammond, J. Am. Chem. Soc., 77 (1955) 334.
42 J.P. McCullough, D.R. Douslin, J.F. Messerly, I.A. Hossenlop, T.C. Kincheloe and G. Waddington, J. Am. Chem. Soc., 79 (1957) 4289.